Theoretical Confirmation of the Low Experimental 3C/3D f-Value Ratio in Fe xvii

C. Mendoza and M. A. Bautista

Theoretical confirmation of the low experimental 3C/3D f-value ratio in Fe XVII

C. Mendoza* and M. A. Bautista

Department of Physics, Western Michigan University, Kalamazoo, MI 49008-5252, USA.†
(Dated: March 9, 2017)

Radiative transition probabilities (A-values) are computed for the Fe XVII L-shell lines in a Breit–Pauli configuration-interaction method with the AUTOSTRUCTURE atomic structure code. It is shown that, by carefully taking into account the fine tuning of the relativistic coupling and $2p$-orbital relaxation, the measured A-values of the M1 and M2 lines and, for the first time, the low $f(3C)/f(3D)$ oscillator-strength ratio are satisfactorily reproduced by theory. The present ratio, $f(3C)/f(3D) = 2.82$, compares well with the measurement of 2.61±0.23 by X-ray laser spectroscopy.

With the advent of the *Chandra* and *XMM-Newton* space telescopes in 1999, the L-shell emission lines ($n = 3 \rightarrow 2$) from 16-time ionized Fe XVII are regular and dominant features in the X-ray spectra of a wide variety of hot (1–7 MK) astronomical entities [1]. However, their plasma diagnostic potential has been marred right from the outset by stubborn mismatches in the spectral models, in particular a weaker-than-predicted resonance line, which are believed to be due to inaccurate atomic structure [2]. A standing discrepancy between the experimental and theoretical electron impact excitation cross sections has neither been fully explained [3–5], but in any case, electron correlation effects in the ionic targets have been shown to be dominant [2, 6]. The view on questionable radiative rates has been recently reinforced by a recent laboratory measurement of the leading oscillator-strength (f-value) ratio using X-ray laser spectroscopy, which is 3.6σ lower than hitherto numerous theoretical efforts (see [7] and references therein). It is shown here for the first time that, by both fine tuning the relativistic coupling and including orbital relaxation effects in the atomic model, the experimental f-value ratio can be theoretically reproduced to within the quoted uncertainty. Consequently, this accord obviates the need to consider nonlinear dynamical modeling [8] or non-equilibrium plasma effects [9].

As specified in Fig. 1, the lines we are referring to arise from the $2p^53s$ and $2p^53d$ excited configurations, and in a similar fashion to the He-like triplet [10], the attractive diagnostic capabilities emerge from their quantum mechanical diversity: 3C and 3G are electric dipole allowed lines, the former being the resonance line; 3D, 3E, and 3F are spin-forbidden electric dipole lines (intercombination lines); and M1 and M2 are respectively magnetic dipole and quadrupole forbidden lines. The radiative rates (A-values) of the latter two have been measured in an electron beam ion trap at $A(\text{M1}) = (1.45 \pm 0.15) \times 10^4$ s^{-1} [11] and $A(\text{M2}) = (2.04^{+0.03}_{-0.09}) \times 10^5$ s^{-1} [12], while the unexpectedly low experimental f-value ratio is $f(3C)/f(3D) = 2.61 \pm 0.23$ [7].

The central theoretical issue in this controversy is the well-known difficulty in obtaining accurate f-values for intercombination lines; not better exemplified than with the systematic studies of the $1s^22s^2\ ^1S_0 - 1s^22s2p\ ^3P_1^o$
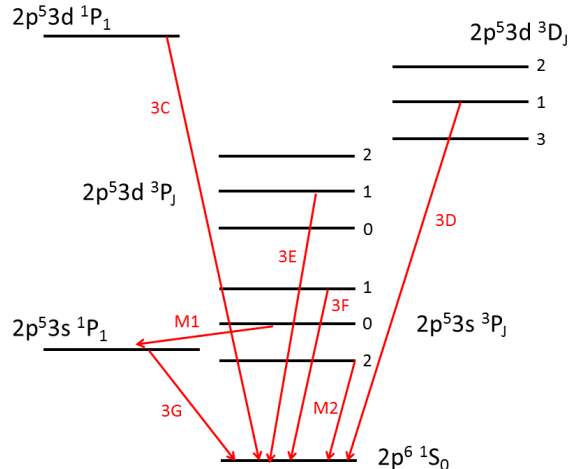

FIG. 1. Fe XVII energy-level diagram (not drawn to scale) showing the spectral lines of interest.

transition in the Be isoelectronic sequence [13–18], in particular in the lowly ionized member C III. Among the many details that need to be painstakingly addressed, the following stand out: slowly convergent configuration-interaction (CI) expansions to account for valence–valence and core–valence (dipole polarizability of the $1s^2$ shell) correlations that require single, double and, in some cases, triple and quadrupole excitations in electron configurations bearing orbitals with principal quantum number $n \leq 9$ [13–18]; relativistic wave functions that undergo strong cancellation effects that demand very precise level-energy separations [16, 18], in particular $\Delta E(2s2p\ ^3P_1^o, 2s2p\ ^1P_1^o)$, which in some methods are only attained by small empirical energy corrections in a procedure referred to as *fine tuning* [14, 19]; large differences between the length and velocity f-value gauges that indicate wave functions far from their exact form [16]; orbital relaxation effects whereby the $2p$ orbital of the $^3P^o$ state appears to be more contracted than that of the $^1P^o$ [15, 16]; and theoretical A-values for the C III 1909 Å intercombination line that lied consistently $\sim 20\%$ below a radio-frequency ion trap measurement [20], discrepancy that was finally resolved with a more precise experimental result in an ion storage ring [21].

In the present computations of the Fe XVII L lines, we follow the well-honed Be-sequence script with a Breit–Pauli CI (BPCI) method examining each of the aforementioned problems. CI wave functions of the type

$$\psi = \sum_i c_i \phi_i \qquad (1)$$

are determined with the AUTOSTRUCTURE atomic structure code [22, 23] using the Breit–Pauli Hamiltonian

$$H_{\rm bp} = H_{\rm nr} + H_{\rm 1b} + H_{\rm 2b} \qquad (2)$$

where $H_{\rm nr}$ is the usual non-relativistic Hamiltonian. The one-body relativistic operator $H_{\rm 1b}$ represents the spin–orbit interaction and the non-fine-structure mass-variation and one-body Darwin corrections. The two-body Breit operator $H_{\rm 2b}$ includes, on the one hand, the fine-structure spin–other-orbit, mutual spin–orbit, and spin–spin terms, and on the other, the non-fine-structure counterparts: spin–spin contact; two-body Darwin; and orbit–orbit. The ϕ_i configuration functions are built up from single-electron orbitals $P_{nl}(r)$ constructed by diagonalizing $H_{\rm nr}$ with a statistical Thomas–Fermi–Dirac–Amaldi model potential $V[\lambda(nl)]$, where the $\lambda(nl)$ scaling parameters are optimized variationally by minimizing suitable combinations of the LS term energies [24].

Fine tuning is implemented by means of term energy corrections (TEC) [25, 26], where the relativistic wave function $\psi_i(R)$ is expressed as a perturbation expansion in terms of the non-relativistic functions $\psi_i(NR)$:

$$\psi_i({\rm R}) = \psi_i({\rm NR})$$
$$+ \sum_{j \neq i} \psi_j({\rm NR}) \cdot \frac{\langle \psi_j({\rm NR})|H_{\rm 1b} + H_{\rm 2b}|\psi_i({\rm NR})\rangle}{E_i({\rm NR}) - E_j({\rm NR})} \cdots , \quad (3)$$

the $E_i({\rm NR})$ and $E_j({\rm NR})$ being adjusted with empirical TEC so as to compute the denominator of Eq. 3 with the experimental energy differences.

Orbital relaxation effects are amply discussed in [27], and with regards to the Ne-like ions, they have been studied in relation to the properties of K-vacancy states in Fe XVII [28] and in the dielectronic recombination of Mg III [29]. In AUTOSTRUCTURE the electron configurations of a particular atomic model usually share a common set of orthogonal orbitals, but orbital relaxation can be introduced by assigning each configuration an independent set of non-orthogonal orbitals for which the overlap integrals are neglected [29]. The effects on the rates due to the 2p-orbital relaxation that occurs in the transition between the L-vacancy states and the spherically symmetric, closed-shell ground state are thus examined.

The following four atomic models are considered in order to study the impact of CI and orbital relaxation on the radiative rates.

Mod1: The ion is represented by electron configurations displaying single and double excitations within the $n = 3$ complex: $2s^2 2p^6$; $2s^2 2p^5 n\ell$; $2s 2p^6 n\ell$; $2s^2 2p^4 n\ell n\ell'$; $2s 2p^5 n\ell n\ell'$, and $2p^6 n\ell n\ell'$ with $\ell \leq 2$ and $\ell' \leq 2$. Orbitals are assumed orthogonal.

Mod2: As Mod1 plus electron configurations displaying single and double excitations within the $n \leq 4$ complexes: $2s^2 2p^5 n'\ell$; $2s 2p^6 n'\ell$; $2s^2 2p^4 n\ell n'\ell'$; $2s 2p^5 n\ell n'\ell'$, and $2p^6 n\ell n'\ell'$ with $n' = 4$, $\ell \leq 2$ and $\ell' \leq 2$. Orbitals are assumed orthogonal.

Mod3: As Mod1 but with non-orthogonal orbitals.

Mod4: As Mod3 but with independently optimized $\overline{2p}$ and $\overline{\overline{2p}}$ orbitals in the $2s^2 \overline{2p}^6$, $2s^2 \overline{2p}^5 3s$, and $2s^2 \overline{\overline{2p}}^5 3d$ configurations.

The $\lambda(1s)$ and $\lambda(2\ell)$ scaling parameters in Mod1 are optimized by variationally minimizing the $1s^2 2s^2 2p^6\ ^1S$ ground-state energy, while the $\lambda(3\ell)$ are obtained by minimizing the energy sum of the spectroscopic terms of $1s^2 2s^2 2p^5 3\ell$ with $L = 0$ for even-parity and $L < 4$ for odd-parity configurations. This scheme accounts for CI in the wave functions of the ground level ($J = 0$) and the excited states of interest ($J \leq 2$). In Mod2 the $\lambda(4\ell)$ with $\ell \leq 2$ are optimized on the energy sum of terms from $1s^2 2s^2 2p^6$ and $1s^2 2s^2 2p^5 3\ell$ previously considered. The resulting scaling parameters are listed in Table I.

TABLE I. Optimized orbital scaling parameters $\lambda(nl)$.

$\lambda(nl)$	Mod1	Mod2	Mod4
$1s$	1.3837	1.3837	1.3837
$2s$	1.0699	1.0699	1.0699
$2p$	1.0051	1.0051	1.0051
$3s$	1.2600	1.2600	1.2600
$3p$	1.0990	1.0990	1.0990
$3d$	1.0875	1.0875	1.0875
$4s$		1.1732	
$4p$		1.0740	
$4d$		1.0758	
$\overline{2p}$			1.1100
$\overline{\overline{2p}}$			1.2400

For the levels shown in Fig. 1, *ab-initio* computed energies from Mod1 and Mod2 are compared with experiment in Table II. The spectroscopic data have been derived from recent wavelength measurements [11, 30–32]. It is shown that the spectroscopic values are reproduced to better than 4 eV with Mod1 while there are no significant improvements with Mod2. *A*-values are then calculated by applying TEC and wavelength corrections, those obtained with Mod1 and Mod2 being listed in Table III. The agreement of these two approximations for the whole transition array is within 5%, and with the experimental M2 and M1 *A*-values somewhat better (see Table IV). As also given in Table IV, Mod1 yields $f(3G)/f(3F) = 1.36$ and $f(3C)/f(3D) = 3.75$

which compare closely to 1.35 and 3.77, respectively, in Mod2. However, such $f(3C)/f(3D)$ theoretical predictions maintain the typical ($\sim 44\%$) discrepancy with experiment.

TABLE II. Comparison of experimental and present theoretical level energies (eV) for Fe XVII. [a]Ref. [11]. [b]Ref. [30]. [c]Ref. [31]. [d]Ref. [32]. Experimental mislabels for some levels have been corrected.

i	Level	Expt	Mod1	Mod2	Mod3	Mod4
1	$2p^6\ ^1S_0$	000.00	000.00	000.00	000.00	000.00
2	$2p^53s\ ^3P_2^o$	725.12^a	727.84	727.71	732.75	726.42
3	$2p^53s\ ^1P_1^o$	727.07^a	729.79	729.64	734.82	728.46
4	$2p^53s\ ^3P_0^o$	737.78^a	740.01	739.94	744.66	739.06
5	$2p^53s\ ^3P_1^o$	739.02^a	741.26	741.17	746.01	740.37
6	$2p^53d\ ^3P_0^o$	801.37^b	804.17	804.49	808.62	803.31
7	$2p^53d\ ^3P_1^o$	802.33^c	805.13	805.45	809.57	804.28
8	$2p^53d\ ^3P_2^o$	804.14^b	806.96	807.30	811.41	806.11
9	$2p^53d\ ^3D_3^o$	807.80^b	810.79	811.16	815.32	809.70
10	$2p^53d\ ^3D_1^o$	812.41^d	815.60	815.90	820.15	814.61
11	$2p^53d\ ^3D_2^o$	818.51^b	820.87	821.23	825.11	821.02
12	$2p^53d\ ^1P_1^o$	825.77^d	829.92	829.97	834.81	829.02

TABLE III. Present A-values (s^{-1}) for the L lines of Fe XVII.

Id	j	i	λ (Å)	Mod1	Mod2	Mod3	Mod4
M2	2	1	17.099	2.10E+05	2.12E+05	3.01E+05	2.04E+05
3G	3	1	17.053	9.26E+11	9.44E+11	1.21E+12	9.07E+11
M1	4	3	1158.4	1.48E+04	1.47E+04	1.59E+04	1.57E+04
3F	5	1	16.777	7.03E+11	7.23E+11	1.06E+12	7.69E+11
3E	7	1	15.453	1.11E+11	1.06E+11	1.19E+11	1.31E+11
3D	10	1	15.261	6.34E+12	6.09E+12	6.77E+12	7.89E+12
3C	12	1	15.014	2.46E+13	2.37E+13	2.88E+13	2.30E+13

Furthermore, for the electric dipole transitions (both allowed and intercombination), the f-value accord between the length and velocity formulations is in both Mod1 and Mod2 within 3% except for the 3F line where it deteriorates, though not unreasonably, to 12% and 9%, respectively. All these results lead to the conclusion that the theoretical $f(3C)/f(3D)$ discrepancy with experiment is not due to a slowly convergent CI expansion.

Before testing the sensitivity of the radiative data to orbital relaxation, we firstly examine the general outcome of implementing an atomic basis of non-orthogonal orbitals, namely Mod3, by adopting the same configuration expansion and scaling parameters as Mod1 (see Table I) but with the orthogonality condition removed. It is seen in Table II that, when the Mod3 level energies are compared with experiment, the discrepancies relative to those of Mod1 increase by a factor of 2–3. Also, as shown in Table III, the A-values for the whole transition array are significantly higher in Mod3, in particular for the M2 (43%), 3G (31%), and 3F (51%) lines, and the

f-value ratios do not change much: $f(3C)/f(3D) = 4.11$ and $f(3G)/f(3F) = 1.19$. Moreover, although the electric dipole length f-values increase accordingly with the A-values, the velocity f-values remain close ($\lesssim 8\%$) to those of Mod1; therefore, the good agreement of the f-value length–velocity gauges in Mod1 and Mod2 is lost in Mod3.

In order to test orbital relaxation effects, we implement the Mod4 model which is in fact similar to Mod3 (i.e., a CI expansion spanning the $n = 3$ complex with non-orthogonal orbitals), but now the $\lambda(2p)$ scaling parameter of each of the $2p^6$, $2p^53s$, and $2p^53d$ configurations is varied independently. It is thus found that the A-values are in general sensitive to small changes of the scaling parameters, and if the TEC are jointly implemented with a judicious $\lambda(2p)$ selection, it is possible to reduce the $f(3C)/f(3D)$ ratio to the experimental value or even lower. The basic question is then how to adopt $2p$-orbital optimization criteria with enough theoretical rigor such that they can be applied to any member of the Ne isoelectronic sequence. We must admit that in such a quest the reported measurements of the Fe XVII M1 and M2 A-values and $f(3C)/f(3D)$ ratio proved to be invaluable.

After much trial and error but always trying to comply with the radiative data measurements, we arrived at the conclusion that the prevailing $2p$-orbital optimization criterion follows that previously emphasized for the Be sequence [15, 19]: the accuracy of the terms

$$\frac{\langle 2p^53s\ ^3P_1^o|H_{1b} + H_{2b}|2p^53s\ ^1P_1^o\rangle}{\Delta E(2p^53s\ ^3P_1^o, 2p^53s\ ^1P_1^o)} \quad (4)$$

and

$$\frac{\langle 2p^53d\ ^3D_1^o|H_{1b} + H_{2b}|2p^53d\ ^1P_1^o\rangle}{\Delta E(2p^53d\ ^3D_1^o, 2p^53d\ ^1P_1^o)} \quad (5)$$

that regulate the intersystem relativistic mixing (see Eq. 3).

Recapitulating, in Mod4 the three spectroscopic configurations $\overline{2p}^6$, $\overline{2p}^53s$, and $\overline{\overline{2p}}^53d$ now include two new $\overline{2p}$ and $\overline{\overline{2p}}$ orbitals that are then optimized as follows:

- $\lambda(\overline{2p})$ is optimized by equating the theoretical energy separation $\Delta E(\overline{2p}^53s\ ^1P_1^o, \overline{2p}^53s\ ^3P_1^o)$ to the spectroscopic value;

- $\lambda(\overline{\overline{2p}})$ is optimized such that the theoretical energy separation $\Delta E(\overline{\overline{2p}}^53d\ ^3D_1^o, \overline{\overline{2p}}^53d\ ^1P_1^o)$ is the closest to the spectroscopic value since, as shown in Fig. 2, the curve goes through a higher minimum.

The optimized values of $\lambda(\overline{2p})$ and $\lambda(\overline{\overline{2p}})$ are listed in Table I. It must be noted that the $\overline{2p}^6$ and $\overline{2p}^53s$ configurations share a common $\overline{2p}$ orbital as it is found that, if they are assumed independent, the optimized

TABLE IV. Comparison of experimental and theoretical A-values and f-value ratios for Fe XVII. [a]Electron beam ion trap [11, 12]. [b]X-ray laser spectroscopy [7]. [c]MBPT [33]. [d]MCDHF-RCI [34]. [e]FAC [12]. [f]MBPT and FAC [35]. [g]BPCI [36]. [h]MBPT and RCI [32].

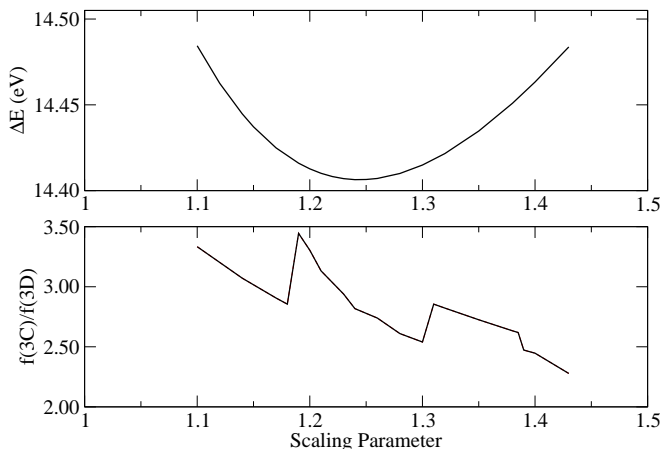| Parameter	Experiment	Mod1	Mod2	Mod4	Other recent theory
$A(M2)$ (s^{-1})	$(2.04^{+0.03}_{-0.09})$E+5[a]	2.10E+5	2.12E+5	2.04E+5	2.06E+5,[c] 2.08E+5,[d] 2.06E+5[e]
$A(M1)$ (s^{-1})	(1.45 ± 0.15)E+4[a]	1.48E+4	1.47E+4	1.57E+4	1.56E+4,[c] 1.59E+4,[d] 1.62E+4,[f] 1.58E+4,[f] 1.55E+4[f]
$f(3G)/f(3F)$		1.36	1.35	1.22	1.22,[c] 1.20,[d] 1.15[g]
$f(3C)/f(3D)$	2.61 ± 0.23[b]	3.75	3.77	2.82	3.48,[c] 3.56,[d] 3.50,[g] 3.96,[h] 3.74,[h] 3.68,[h] 3.44[h]

FIG. 2. $\Delta E(\overline{\overline{2p}}^5 3d\ ^3D_1^o, \overline{\overline{2p}}^5 3d\ ^1P_1^o)$ energy difference (top panel) and $f(3C)/f(3D)$ ratio (bottom panel) as a function of the $\lambda(\overline{\overline{2p}})$ scaling parameter. The spectroscopic value of $\Delta E = 13.36$ eV is never reached, but the procedure allows an optimized value of $\lambda(\overline{\overline{2p}}) = 1.24$ to be determined. $f(3C)/f(3D)$ are obtained after the TEC are applied resulting in a value of 2.82 with the optimized scaling parameter.

scaling parameters are fairly close while, in contrast, the $\overline{\overline{2p}}$ orbital in $\overline{\overline{2p}}^5 3d$ is definitely more diffuse. It may be appreciated in Fig. 2 that the $\lambda(\overline{\overline{2p}})$ optimization in the range $1.10 \leq \lambda(\overline{\overline{2p}}) \leq 1.40$ causes a variation of $\Delta E(\overline{\overline{2p}}^5 3d\ ^3D_1^o, \overline{\overline{2p}}^5 3d\ ^1P_1^o)$ of only $\lesssim 0.08$ eV, and hence, the spectroscopic separation of 13.36 eV is never reached. On the other hand, the effect of this orbital variation on the $f(3C)/f(3D)$ ratio once the TEC are applied is remarkable: $2.3 \lesssim f(3C)/f(3D) \lesssim 3.5$. Since the TEC are adjusted to the spectroscopic term centroids, the discontinuities observed in $f(3C)/f(3D)$ (see Fig. 2) are a result of the corresponding changes in the energies of the fine-structure levels with $J = 2$ and $J = 3$, and provide a measure of the intricate level coupling of the $3 \rightarrow 2$ transition array in Fe XVII.

The resulting Mod4 level energies are listed in Table II finding significant improvements with respect to Mod3. The A-values obtained in Mod4 are given in Table III, where it is shown that those for the M2, 3G, and 3F lines are reduced by around 30% and for 3C by 20% with

respect to Mod3 while the M1 A-value is hardly modified; those for the 3E and 3D intercombination lines are respectively increased by 10% and 17%. Moreover, it is found that the length–velocity f-value agreement for the dipole lines is fully restored in Mod4 to the Mod1 level: $\sim 2\%$ except for 3F (8%).

The present Mod1, Mod2, and Mod4 radiative data are compared in Table IV with experiment and calculations performed in the past decade using a variety of numerical methods: relativistic CI [32]; many-body perturbation theory (MBPT) [32, 33, 35]; the flexible atomic code (FAC) [12, 35]; multiconfiguration Dirac–Hartree–Fock combined with a relativistic CI method (MCDHF-RCI) [34]; and the same BPCI method as the present [36]. The Mod4 M2 A-value is in very good agreement with both experiment and previous theoretical estimates; however, the Mod4 M1 A-value is a little higher than experiment (still within the experimental uncertainty), Mod1, and Mod2 but in very good accord with the other theoretical data. Mod1 and Mod2 predict $f(3G)/f(3F)$ ratios that are 10% higher than the rest of the theoretical results. Lastly, only Mod4 yields a $f(3C)/f(3D)$ ratio in agreement with experiment.

We have therefore demonstrated that it is possible to reproduce the low experimental $f(3C)/f(3D)$ ratio in Fe XVII if detailed attention is given to the relativistic coupling between levels with $J = 1$ (see Eqs. 4–5), which can be achieved by jointly recurring to fine tuning and an orbital optimization scheme that primarily addresses the precise representation of this coupling. Our best theoretical value of 2.82 is in agreement with the experimental value of 2.61 ± 0.23 to within the error bars. We have also devised a theoretical procedure that would enable the treatment of these subtle effects in the calculation of more reliable radiative data for other Ne-like ions without having to rely on measurements (except the experimental level energies needed for TEC), which in the present work were of vital importance to actually master it.

––––––––––

[*] Also Emeritus Research Fellow, Venezuelan Institute for Scientific Research, Caracas, Venezuela.

[†] claudio.mendozaguardia@wmich.edu

[1] F. B. S. Paerels and S. M. Kahn, Annu. Rev. Astron. Astr. **41**, 291 (2003).

[2] M. F. Gu, arXiv:0905.0519.

[3] G. V. Brown, P. Beiersdorfer, H. Chen, J. H. Scofield, K. R. Boyce, R. L. Kelley, C. A. Kilbourne, F. S. Porter, M. F. Gu, S. M. Kahn, and A. E. Szymkowiak, Phys. Rev. Lett. **96**, 253201 (2006).

[4] V. K. Nikulin and M. B. Trzhaskovskaya, Phys. Rev. Lett. **108**, 139301 (2012).

[5] G. V. Brown and P. Beiersdorfer, Phys. Rev. Lett. **108**, 139302 (2012).

[6] K. B. Fournier and S. B. Hansen, Phys. Rev. A **71**, 012717 (2005).

[7] S. Bernitt, G. V. Brown, J. K. Rudolph, R. Steinbrügge, A. Graf, M. Leutenegger, S. W. Epp, S. Eberle, K. Kubiček, V. Mäckel, M. C. Simon, E. Träbert, E. W. Magee, C. Beilmann, N. Hell, S. Schippers, A. Müller, S. M. Kahn, A. Surzhykov, Z. Harman, C. H. Keitel, J. Clementson, F. S. Porter, W. Schlotter, J. J. Turner, J. Ullrich, P. Beiersdorfer, and J. R. Crespo López-Urrutia, Nature **492**, 225 (2012).

[8] N. S. Oreshkina, S. M. Cavaletto, C. H. Keitel, and Z. Harman, Phys. Rev. Lett. **113**, 143001 (2014).

[9] S. D. Loch, C. P. Ballance, Y. Li, M. Fogle, and C. J. Fontes, Astrophys. J. **801**, L13 (2015).

[10] D. Porquet, J. Dubau, and N. Grosso, Space Sci. Rev. **157**, 103 (2010).

[11] P. Beiersdorfer, J. R. Crespo López-Urrutia, and E. Träbert, Astrophys. J. **817**, 67 (2016).

[12] J. R. Crespo López-Urrutia and P. Beiersdorfer, Astrophys. J. **721**, 576 (2010).

[13] J. Fleming, A. Hibbert, and R. P. Stafford, Phys. Scripta **49**, 316 (1994).

[14] J. Fleming, K. L. Bell, A. Hibbert, N. Vaeck, and M. R. Godefroid, Mon. Not. R. Astron. Soc. **279**, 1289 (1996).

[15] C. Froese Fischer, Phys. Scripta **49**, 323 (1994).

[16] A. Ynnerman and C. Froese Fischer, Phys. Rev. A **51**, 2020 (1995).

[17] C. Froese Fischer and G. Gaigalas, Phys. Scripta **56**, 436 (1997).

[18] P. Jönsson and C. Froese Fischer, Phys. Rev. A **57**, 4967 (1998).

[19] A. Hibbert, Phys. Scripta **T65**, 104 (1996).

[20] V. H. S. Kwong, Z. Fang, T. T. Gibbons, W. H. Parkinson, and P. L. Smith, Astrophys. J. **411**, 431 (1993).

[21] J. Doerfert, E. Träbert, A. Wolf, D. Schwalm, and O. Uwira, Phys. Rev. Lett. **78**, 4355 (1997).

[22] W. Eissner, M. Jones, and H. Nussbaumer, Comput. Phys. Commun. **8**, 270 (1974).

[23] N. R. Badnell, Comput. Phys. Commun. **182**, 1528 (2011).

[24] W. Eissner and H. Nussbaumer, J. Phys. B - At. Mol. **2**, 1028 (1969).

[25] C. J. Zeippen, M. J. Seaton, and D. C. Morton, Mon. Not. R. Astron. Soc. **181**, 527 (1977).

[26] C. Mendoza and C. J. Zeippen, Mon. Not. R. Astron. Soc. **198**, 127 (1982).

[27] R. D. Cowan, *The theory of atomic structure and spectra* (University of California, Berkeley, 1981).

[28] C. Mendoza, T. R. Kallman, M. A. Bautista, and P. Palmeri, Astron. Astrophys. **414**, 377 (2004).

[29] J. Fu, T. W. Gorczyca, D. Nikolic, N. R. Badnell, D. W. Savin, and M. F. Gu, Phys. Rev A **77**, 032713 (2008).

[30] C. Jupén and U. Litzén, Phys. Scripta **30**, 112 (1984).

[31] G. V. Brown, P. Beiersdorfer, D. A. Liedahl, K. Widmann, and S. M. Kahn, Astrophys. J. **502**, 1015 (1998); **532**, 1245 (2000).

[32] J. A. Santana, J. K. Lepson, E. Träbert, and P. Beiersdorfer, Phys. Rev. A **91**, 012502 (2015).

[33] K. Wang, Z. B. Chen, R. Si, P. Jönsson, J. Ekman, X. L. Guo, S. Li, F. Y. Long, W. Dang, X. H. Zhao, R. Hutton, C. Y. Chen, J. Yan, and X. Yang, Astrophys. J. Suppl. S. **226**, 14 (2016).

[34] P. Jönsson, P. Bengtsson, J. Ekman, S. Gustafsson, L. B. Karlsson, G. Gaigalas, C. Froese Fischer, D. Kato, I. Murakami, H. A. Sakaue, H. Hara, T. Watanabe, N. Nakamura, and N. Yamamoto, Atom. Data Nucl. Data **100**, 1 (2014).

[35] P. Beiersdorfer, M. Obst, and U. I. Safronova, Phys. Rev. A **83**, 012514 (2011).

[36] C. Zhou, J.-J. Cao, L. Liang, G. H. Yu, Z.-M. Wang, and H.-Y. He, Acta Phys. Pol. A **129**, 1109 (2016).